Cell, Volume *139*

Supplemental Data

Stringent Specificity in the Construction of a GABAergic Presynaptic Inhibitory Circuit

J. Nicholas Betley, Christopher V.E. Wright, Yoshiya Kawaguchi, Ferenc Erdélyi, Gábor Szabó, Thomas M. Jessell, and Julia A. Kaltschmidt

Supplemental Experimental Procedures

Mouse Strains

The following mouse strains were used in this study: *Gad65::*^{N45}GFP (Lopez-Bendito et al., 2004), *Hb9::*eGFP (Wichterle et al., 2002), *ROSA::Φ*LacZ (Soriano 1999) (in all strains, *Φ* indicates a *loxP.STOP.loxP* cassette), *ROSA::Φ*YFP (Srinivas et al., 2001), *Thy1::Φ*YFP (line2) and *Thy1::Φ*YFP (line15) (Buffelli et al., 2003), *Tau::Φ*mGFP (Hippenmeyer et al., 2005), *Emx1::*Cre (Gorski et al., 2002), *En1::*Cre (Kimmel et al., 2000), *Ht-PA::*Cre (Pietri et al., 2003), *Ptf1a::*Cre (Kawaguchi et al., 2002), *Pv*::Cre (Hippenmeyer et al., 2005), *BDNF* (Ernfors et al., 1994), conditional *BDNF* (Rios et al., 2001), *BDNF::*LacZ (Bennett et al., 1999), *Er81 ex11 taulacZ* (Arber et al., 2000), conditional *TrkB* (Minichiello et al., 1999), *Isl2::Φ*Dta (Yang et al., 2001).

Histochemistry

In situ hybridization histochemistry was performed using probes generated by polymerase chain reaction (PCR) from mouse spinal cord and brain cDNA, with the antisense probe length ranging from 500-1200 base pairs. *In situ* hybridization histochemistry was performed on 10-15 μm cryostat sections as previously described (Arber et al., 2000) and double fluorescent *in situ* hybridization histochemistry was performed as previously described (Price et al., 2002).

Immunohistochemistry

Antibodies against synaptic proteins were generated in guinea pigs, rabbits and rats using the following peptide sequences: GAD65: SEDGSADPENPGTARAWSQVAQKFTGGIGNKLSALLYGDSGC and CRTLEDNEERMSRLSK, GAD67: ENSDQGARFRRTETDC, Shank1a: CSGPIYPGLFDIRSS, vGAT: AEPPVEGDIHYQR and vGlut1: CGATHSTVQPPRPPPPVRDY.

Additional antibodies: mouse anti-Bassoon 1:4000 (Stressgen Bioreagents), goat anti-ß-gal 1:1000 (Biogenesis), chick anti-ß-gal 1:500 (Chemicon Int'l), rabbit anti-Calbindin 1:2000 (Swant), goat anti-ChAT 1:200 (Chemicon Int'l), rabbit anti-Enkephalin, Pre Pro 1:1000 (Neuronomics), rabbit anti-$GABA_A$ α6 1:1000 (Chemicon Int'l), mouse anti-$GABA_A$ β2/3 1:500 (Upstate), rabbit anti-GAD65 1:1500 (Chemicon Int'l), mouse anti-GAD67 1:10000 (Chemicon Int'l), mouse anti-Geph 1:8000 (Synaptic Systems), rabbit anti-GFP 1:2000 (Molecular Probes, Invitrogen), sheep anti-GFP 1:2000 (Biogenesis), rabbit anti-GluR2/3 1:50 (Chemicon Int'l), rabbit anti-NPY 1:1000 (Abcam), mouse anti-PSD95 K28/43 1:1000 (Upstate), goat anti-Pv 1:2000 (Swant), rabbit anti-Shank1a 1:1000 (Chemicon Int'l), mouse anti-SV2 1:200 (Developmental Studies Hybridoma Bank), rabbit anti-Synapsin 1 1:1000 (Chemicon Int'l), mouse anti-Synaptotagmin 1 (ASV 48) 1:50-1:500 (Developmental Studies Hybridoma Bank), goat anti-vAChT 1:2000 (Chemicon Int'l), mouse anti-vGAT 1:4000 (Synaptic Systems), guinea pig anti-vGlut1 1:20000 (Chemicon Int'l), rabbit anti-vGlut1 1:1000 (Synaptic Systems) and guinea pig anti-vGlut2 1:3000 (Chemicon Int'l).

Epitope unmasking was performed for immunohistochemistry against PSD95 and GluR2/3, by incubating fresh frozen tissue in -20°C methanol for 10 minutes before the staining protocol.

Determination of GABAergic bouton size

Distribution of the volumes of GABAergic boutons and varicosities in ventral spinal cord. $Gad65^{+}$ terminals contacting sensory terminals (pre: s) have a mean volume of $0.24 \pm 0.04\ \mu m^3$ (n = 103 boutons; 3 mice). The varicosities of *Ptf1a::*Cre ; *Φ*FP^{+}-marked GABApre axons (see text and Figure 3) that contact motor neurons (pre: mn) have a mean volume of $1.46 \pm 0.15\ \mu m^3$ (n = 104 boutons; 3 mice). $Gad67^{+}$, $Gad65^{off}$ terminals contacting motor neurons (post: mn) have a mean bouton volume of $0.80 \pm 0.08 \mu m^3$ (n = 102 boutons; 3 mice). The varicosities of *Ptf1a::*Cre ; *Φ*FP^{+}-marked GABApre axons that contact motor neurons and ventral interneurons in *Er81* mutants (pre: $Er81^{-/-}$) have a mean bouton volume of $1.46 \pm 0.16 \mu m^3$ (n = 103 boutons; 3 mice). In each comparison, except between pre: mn contacts in the wild type and *Er81* mutant background (which are not significantly different), differences in volume are significant at $p < 0.0001$ (Mann-Whitney U Test).

Determination of GABApre synaptic specificity index

Images of $vGlut1^{+}$ or $GAD67^{+}$ terminals on GFP^{+} motor neurons were obtained on BioRad MRC 1024 or Zeiss LSM510 Meta confocal microscopes and reconstructed with Neurolucida 8 (MicroBrightField Bioscience). The number of synapses in relation to the motor neuron surface area (comprised of traces of motor neuron cell body and proximal dendrites) was scored in confocal z-stacks (0.5 μm step size).

To determine the surface area (SA) of $vGlut1^{+}$ terminals, we approximated their shape as an oblate ellipsoid. The equatorial radius along the x- (a) and y-axis (b) of terminals cut in a horizontal plane and the polar radius along the z-axis (c) of terminals cut in a perpendicular plane were measured using Neurolucida 8. The SA of $vGlut1^{+}$ terminals was calculated using a = b (oblate ellipsoid) as a maximal approximation for a scalene ellipsoid (the typical shape of a $vGlut1^{+}$ terminal), using the SA formula for an oblate ellipsoid ($SA = 2\pi (a^2 + c^2 [\text{arctanh} (\sin (Œ) / \sin (Œ)]$) with $Œ = \arccos (c / a)$). Measurement of a (1.2 μm) and c dimensions of terminals cut in vertical plane gives an estimate c = 0.4a, or 0.5 μm.

From these values, we calculate the mean SA of a vGlut1$^+$ proprioceptive sensory terminal as 11.8 ± 1.1 μm^2 (n = 327 terminals; 7 mice). Since one face of vGlut1$^+$ terminals contacts motor neurons, the available SA for GABApre contact is reduced by ~1 / 3, giving an available SA of 7.9 ± 0.7 μm^2.

The SA of morphologically defined alpha motor neurons was measured using Neurolucida 8 (4769 ± 270 μm^2; n = 6 motor neurons; 3 mice). We traced vGlut1$^+$ terminals on reconstructed motor neurons and found 34 ± 3 vGlut1$^+$ terminals / motor neuron cell body and proximal dendrites (n = 206 vGlut1$^+$ terminals; 3 mice). Therefore the ratio of [motor neuron : vGlut1$^+$ terminal] SA = 4769 / (34 x 7.9) = 17.8.

The number of GAD65$^+$ synapses in contact with vGlut1$^+$ terminals was determined on collapsed confocal z-stacks to be 3.2 ± 0.1 (n = 126 GAD65$^+$ terminals; 3 mice). Since there are 34 vGlut1$^+$ terminals / motor neuron, we calculated the number of GAD65$^+$ synapses / motor neuron = 3.2 x 34 = 108.8. Thus Gad65$^+$ terminals exhibit a specificity index (108.8 x 17.8) of 1937. The number of Gad67$^+$ synapses in contact with motor neurons was estimated to be 88 / motor neuron. Thus Gad67$^+$ terminals exhibit a specificity index of (88 x (1 / 17.8)) = 4.9.

Quantitation of GABApre axonal retraction

The density of YFP$^+$ axons and boutons was calculated by converting an image of a single optical section taken at airy units into a binary image (threshold function), where all labeling was converted to a value of 1 and all area devoid of labeling was converted to a value of 0. The number of pixels with a value of 1 divided by the total number of pixels gives the YFP process density. Differences between wild type and mutant density are significant at $p < 0.001$ (Mann-Whitney U Test). Values obtained from >100 bouton measurements in 3 or more mice.

Supplemental Results and Discussion

Excluding a temporal basis for GABApre synaptic specificity

The axons of developing GABApost neurons contact motor neurons long before those of GABApre neurons (Saueressig et al., 1999; Alvarez et al., 2005), raising the possibility that selective connectivity might have its origin in a temporal program that reflects the order of axonal arrival in the vicinity of motor neurons. Upon their eventual arrival, GABApre axons might be excluded from contacting motor neurons since all post-synaptic inhibitory space is occupied by the terminals of GABApost neurons and other interneurons. In this temporal scenario, the later arrival of proprioceptive sensory terminals could provide GABApre axons with a much-needed synaptic target that is of no interest to GABApost axons because of their prior synaptic association with motor neurons.

Our analysis of the relationship between GABApre axons and motor neurons argues strongly against this temporal model. We find that *Ptf1a*-marked GABApre axons are able to make early contact with motor neurons as well as sensory terminals. Yet GABApre axons fail to exhibit any sign of pre-synaptic specialization at sites of motor neuron contact, despite the receptivity of motor neurons to other GABAergic inputs (Figure S7A-C, S8). These observations effectively preclude models in which the mature pattern of GABAergic synaptic connectivity results from denial of access of GABApre axons to motor neurons, reinforcing the notion of synaptic recognition specificity.

GABApre axon – motor neuron contacts do not represent functional synapses

By p40, almost all GABApre axonal contacts with motor neurons have been lost, and at this stage the few remaining GFP-labeled varicosities are no longer aligned with $Geph^{+}$ puncta (Figure S8). We find identical results in both wild type and *Pv*::Cre ; *Isl2::Φ*Dta sensory terminal deleted mice (data not shown). These findings indicate that the initial non-functional association between GABApre axons and motor neurons does not persist beyond the first post-natal month. One likely explanation for the

occurrence of these transient GABApre axon-motor neuron contacts is simply that the overall axonal packing density in the vicinity of motor neurons is extremely high, and thus GABApre axons in search of their sensory terminal targets cannot avoid contact with the motor neuron membrane. Our data show that these initial motor neuron contacts never mature into functional synapses, due to a failure of pre-synaptic differentiation and the absence of post-synaptic $GABA_A$ receptors. The fact that we observe motor neuron $Geph^+$ puncta in alignment with some of these GABApre axon contacts raises the possibility that the pre-synaptic axon is capable of initiating some aspects of a post-synaptic differentiation program, even though the motor neuron is incapable of triggering pre-synaptic differentiation. But since $GABA_A$ receptor subunits are not detected post-synaptically, these contacts cannot be functional synapses. Presumably after p30, the rearrangement of axons and neuronal cell bodies that accompanies the maturation of connections in the ventral horn tugs GABApre axons away from their poorly grounded contacts with the motor neuron membrane. Despite all this tugging, GABApre axons remain firmly attached to sensory terminal – a reflection of the specificity and maturation of this synaptic contact.

Since the GABApre axonal contacts with motor neurons are never found as mature synapses, our findings imply that the striking specificity we observe is attained in two stages. *Stage 1: The productive contact stage.* Despite the fact that GABApre axons are able to contact motor neurons and sensory terminals, only sensory terminals induce synaptic differentiation in GABApre axons. This is the basis for our conclusions about high specificity. *Stage 2: Late elimination of non-productive contacts.* Well after the establishment of productive and specific GABApre-sensory terminal contacts, the non-productive GABApre-motor neuron contacts are cleared. But since these contacts were not productive in the first place, this is very different from the idea that synaptic specificity in this system emerges through elimination of productive but ectopic synapses. In this sense, our findings are in stark contrast to studies of synaptic pruning in hippocampus, where there is now compelling evidence that the pruned synapses were functional (Liu et al., 2005).

Evidence that pre-synaptic inhibitory synapses on cutaneous and proprioceptive sensory afferents derive from distinct populations of *Ptf1a*-marked GABAergic interneurons

Cutaneous sensory afferents that convey nociceptive and mechanoreceptive information terminate in the dorsal horn of the spinal cord and also receive axo-axonic inhibitory synapses from GABAergic interneurons (Maxwell and Rethelyi, 1987). These observations raise the issue of whether a single coherent population of GABApre neurons forms pre-synaptic contacts with proprioceptive and cutaneous sensory terminals. Several lines of evidence indicate that distinct classes of spinal GABAergic interneurons form axo-axonic synapses with proprioceptive and cutaneous sensory afferent terminals.

Axonal projection patterns of identified GABAergic interneurons.

Inhibitory interneurons in the intermediate spinal cord, in the position of the GABApre neurons described in our work, send axons ventrally into the motor neuron region but do not send axons into the dorsal horn. Evidence in cat (Bannatyne et al., 2009) has established these features of GABA neuronal projections through intracellular neuronal fills, axonal tracing and transmitter cytochemistry. A similar organization exists in rodents (Watson and Bazzaz, 2001; Hughes et al., 2005). Thus, anatomical evidence argues strongly against the view that the GABApre neurons that contact proprioceptive sensory terminals send axons into the dorsal horn to contact the terminals of cutaneous afferents.

Distinct amino acid transmitter phenotype of GABAergic interneurons that form pre-synaptic contacts with proprioceptive and cutaneous afferents.

Our studies show that the GABAergic interneurons that form pre-synaptic contacts with proprioceptive sensory afferents express GABAergic but not glycinergic transporters. Many studies have shown that most of the GABAergic neurons that form pre-synaptic contacts with cutaneous sensory afferents express both glycinergic and GABAergic neurotransmitter systems (Figure 3; Sutherland et al., 2002). The expression of distinct inhibitory transmitter profiles supports the view that distinct sets of GABA interneurons contact proprioceptive and cutaneous sensory afferent terminals. In addition, there is

considerable evidence that the GABAergic/glycinergic interneurons that contact cutaneous sensory terminals have their cell bodies in laminae I-III of the dorsal horn (Todd and Spike 1993; Todd, 1996; Polgar et al., 1999).

Distinct peptidergic phenotype of GABAergic interneurons that form pre-synaptic contacts with proprioceptive and cutaneous afferents.

Many studies have shown that GABAergic neurons in the superficial dorsal horn that contact cutaneous sensory terminals co-express a variety of neuropeptides, including enkephalin, thyrotropin releasing hormone and neuropeptide Y (Fleming and Todd, 1994; Laing et al., 1994; Polgar et al., 1999). We have found that these peptides are not expressed by the GABApre boutons that contact proprioceptive sensory terminals in the ventral spinal cord, nor are these genes expressed by *Ptf1a*-marked GABApre neurons in the intermediate spinal cord (Figure 3). These observations add further support to the view that the GABApre neurons that contact proprioceptive sensory terminals are molecularly distinct from those that contact cutaneous sensory terminals.

Transcriptional distinctions in GABApre and superficial dorsal horn GABAergic interneurons.

In recent studies we have found that the *Ptf1a*-marked interneuron population comprises several subpopulations that can be distinguished by additional transcriptional markers. In particular, GABAergic interneurons in the superficial dorsal horn that contact cutaneous afferents express Gbx1 and Lmx1/2 but not Lbx1 and Zic4, whereas GABApre interneurons in the intermediate spinal cord that contact proporioceptive terminals express Lbx1 and Zic4 but not Gbx1 and Lmx1/2 (data not shown).

Thus, the GABApre neurons that contact proprioceptive sensory afferents differ from the GABAergic interneurons in the superficial dorsal horn that form axo-axonic synapses with cutaneous sensory endings by virtue of their settling position, axonal projection pattern, and amino acid and peptidergic phenotype. If the GABApre neurons that contact ventral proprioceptive sensory terminals do

form pre-synaptic connections with another sensory target, it is likely to be the terminals of group Ib proprioceptive sensory afferents, which arborize in the intermediate spinal cord, close to the position of GABApre neuronal cell bodies. Indeed, EM studies by Walmsley and others have shown that the pre-synaptic boutons on group Ib afferents have the same features as those on group Ia terminals in contact with motor neurons (Walmsley et al., 1987).

This fact then raises the possibility that GABApre axons refuse to make alternate synaptic contacts with motor neurons in *Er81* mutants because they remain connected to group Ib sensory terminals. But our experiments using the *Pv*::Cre ; *Isl2::Φ*Dta mice, in which all (group Ia plus group Ib) proprioceptive sensory neurons have been killed show that this is not the case. We find the same stringent specificity of GABApre connections in the ventral spinal cord in *Er81* and *Pv::*Cre ; *Isl2::Φ*Dta mice, arguing that the persistence of group Ib afferents in *Er81* mutants (Arber et al., 2000) cannot be the explanation for the synaptic stringency we observe.

Supplemental References

Alvarez, F.J., Jonas, P.C., Sapir, T., Hartley, R., Berrocal, M.C., Geiman, E.J., Todd, A.J., and Goulding, M. (2005). Postnatal phenotype and localization of spinal cord V1 derived interneurons. J. Comp. Neurol. 493, 177-192.

Arber, S., Ladle, D.R., Lin, J.H., Frank, E., and Jessell, T.M. (2000). ETS gene Er81 controls the formation of functional connections between group Ia sensory afferents and motor neurons. Cell 101, 485-498.

Bannatyne, B.A., Liu, T.T., Hammar, I., Stecina, K., Jankowska, E., and Maxwell, D.J. (2009). Excitatory and inhibitory intermediate zone interneurons in pathways from feline group I and II afferents: differences in axonal projections and input. J. Physiol. 587, 379-399.

Bareyre, F.M., Kerschensteiner, M., Misgeld, T., and Sanes, J.R. (2005). Transgenic labeling of the corticospinal tract for monitoring axonal responses to spinal cord injury. Nat. Med. 11, 1355-1360.

Bennett, J.L., Zeiler, S.R., and Jones, K.R. (1999). Patterned expression of BDNF and NT-3 in the retina and anterior segment of the developing mammalian eye. Invest. Ophthalmol. Vis. Sci. 40, 2996-3005.

Buffelli, M., Burgess, R.W., Feng, G., Lobe, C.G., Lichtman, J.W., and Sanes, J.R. (2003). Genetic evidence that relative synaptic efficacy biases the outcome of synaptic competition. Nature 424, 430-434.

Ernfors, P., Lee, K.F., and Jaenisch, R. (1994). Mice lacking brain-derived neurotrophic factor develop with sensory deficits. Nature 368, 147-150.

Fleming A.A., and Todd A.J. (1994). Thyrotropin-releasing hormone- and GABA-like immunoreactivity coexist in neurons in the dorsal horn of the rat spinal cord. Brain Res. 638, 347-351.

Gorski, J.A., Talley, T., Qiu, M., Puelles, L., Rubenstein, J.L., and Jones, K.R. (2002). Cortical excitatory neurons and glia, but not GABAergic neurons, are produced in the Emx1-expressing lineage. J. Neurosci. 22, 6309-6314.

Hippenmeyer, S., Vrieseling, E., Sigrist, M., Portmann, T., Laengle, C., Ladle, D.R., and Arber, S. (2005). A developmental switch in the response of DRG neurons to ETS transcription factor signaling. PLoS Biol. 3, e159**.**

Hughes, D.I., Mackie, M., Nagy, G.G., Riddell, J.S., Maxwell, D.J., Szabo, G., Erdelyi, F., Veress, G., Szucs, P., Antal, M., et al. (2005). P boutons in lamina IX of the rodent spinal cord express high levels of glutamic acid decarboxylase-65 and originate from cells in deep medial dorsal horn. Proc. Natl. Acad. Sci. USA 102, 9038-9043.

Kawaguchi, Y., Cooper, B., Gannon, M., Ray, M., MacDonald, R.J., and Wright, C.V. (2002). The role of the transcriptional regulator Ptf1a in converting intestinal to pancreatic progenitors. Nat. Genet. 32, 128-134.

Kimmel, R.A., Turnbull, D.H., Blanquet, V., Wurst, W., Loomis, C.A., and Joyner, A.L. (2000). Two lineage boundaries coordinate vertebrate apical ectodermal ridge formation. Genes Dev. 14, 1377-1389.

Laing, I., Todd, A.J., Heizmann, C.W., and Schmidt, H.H. (1994). Subpopulations of GABAergic neurons in laminae I-III of rat spinal dorsal horn defined by coexistence with classical transmitters, peptides, nitric oxide synthase or parvalbumin. Neuroscience 61, 123-132.

Liu, X.B., Low, L.K., Jones, E.G., and Cheng, H.J. (2005). Stereotyped axon pruning via plexin signaling is associated with synaptic complex elimination in the hippocampus. J. Neurosci. 25, 9124-9134.

Lopez-Bendito, G., Sturgess, K., Erdelyi, F., Szabo, G., Molnar, Z., and Paulsen, O. (2004). Preferential origin and layer destination of GAD65-GFP cortical interneurons. Cereb. Cortex 14, 1122-1133.

Maxwell, D.J., and Rethelyi, M. (1987). Ultrastructure and synaptic connections of cutaneous afferent fibers in the spinal cord. Trends Neurosci. 10, 117-123.

Minichiello, L., Korte, M., Wolfer, D., Kuhn, R., Unsicker, K., Cestari, V., Rossi-Arnaud, C., Lipp, H.P., Bonhoeffer, T., and Klein, R. (1999). Essential role for TrkB receptors in hippocampus-mediated learning. Neuron 24, 401-414.

Pietri, T., Eder, O., Blanche, M., Thiery, J.P., and Dufour, S. (2003). The human tissue plasminogen activator-Cre mouse: a new tool for targeting specifically neural crest cells and their derivatives in vivo. Dev. Biol. 259, 176-187.

Polgar, E., Shehab, S.A., Watt, C., and Todd, A.J. (1999). GABAergic neurons that contain neuropeptide Y selectively target cells with the neurokinin 1 receptor in laminae III and IV of the rat spinal cord. J Neurosci. 19, 2637-2646.

Price, S.R., De Marco Garcia, N.V., Ranscht, B., and Jessell, T.M. (2002). Regulation of motor neuron pool sorting by differential expression of type II cadherins. Cell 109, 205-216.

Rios, M., Fan, G., Fekete, C., Kelly, J., Bates, B., Kuehn, R., Lechan, R.M., and Jaenisch, R. (2001). Conditional deletion of brain-derived neurotrophic factor in the postnatal brain leads to obesity and hyperactivity. Mol. Endocrinol. 15, 1748-1757.

Saueressig, H., Burrill, J., and Goulding, M. (1999). Engrailed-1 and netrin-1 regulate axon pathfinding by association interneurons that project to motor neurons. Development 126, 4201-4212.

Soriano, P. (1999). Generalized lacZ expression with the ROSA26 Cre reporter strain. Nat. Genet. 21, 70-71.

Srinivas, S., Watanabe, T., Lin, C.S., William, C.M., Tanabe, Y., Jessell, T.M., and Costantini, F. (2001). Cre reporter strains produced by targeted insertion of EYFP and ECFP into the ROSA26 locus. BMC Dev. Biol. 1, 4.

Sutherland, F.I., Bannatyne, B.A., Kerr, R., Riddell, J.S., and Maxwell, D.J. (2002). Inhibitory amino acid transmitters associated with axons in presynaptic apposition in cutaneous primary afferent axons in the cat spinal cord. J. Comp. Neurol. 452, 154-162.

Todd, A.J. (1996). GABA and glycine in synaptic glomeruli of the rat spinal dorsal horn. Eur. J. Neurosci. 8, 2492-2498.

Todd, A.J., and Spike, R.C. (1993) The localization of classical transmitters and neuropeptides within neurons in laminae I-III of the mammalian spinal cord. Prog. Neurobiol. 41, 609-645.

Walmsley, B., Wieniawa-Narkiewicz, E., and Nicol, M.J. (1987). Ultrastructural evidence related to presynaptic inhibition of primary muscle afferents in Clarke's column of the cat. J. Neurosci. 7, 236-243.

Watson, A.H., and Bazzaz, A.A. (2001). GABA and glycine-like immunoreactivity at axoaxonic synapses on 1a muscle afferent terminals in the spinal cord of the rat. J. Comp. Neurol. 433, 335-348.

Wichterle, H., Lieberam, I., Porter, J.A., and Jessell, T.M. (2002). Directed differentiation of embryonic stem cells into motor neurons. Cell 110, 385-397.

Yang, X., Arber, S., William, C., Li, L., Tanabe, Y., Jessell, T.M., Birchmeier, C., and Burden, S.J. (2001). Patterning of muscle acetylcholine receptor gene expression in the absence of motor innervation. Neuron 30, 399-410.

Supplemental Figures

Figure S1

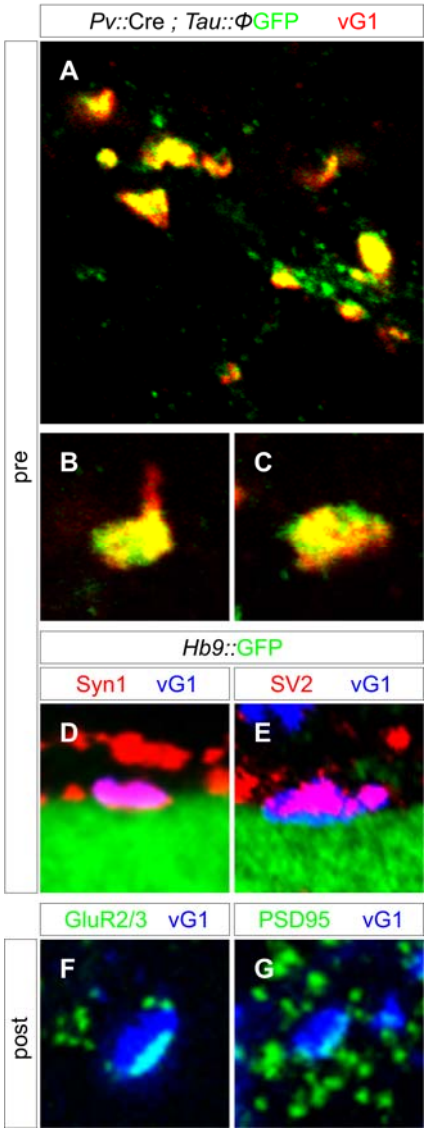

Figure S1. Molecular identification of proprioceptive sensory-motor synapses

(A-C) In *Pv::*Cre *; Tau::Φ*mGFP mice, 95.6 ± 0.9% (n = 971; 3 mice) of vGlut1 $(vG1)^{+}$ terminals in p21 ventral spinal cord express mGFP, establishing their proprioceptive sensory origin. CST neurons, believed to be glutamatergic, have been shown to contact motor neurons in adult mice (Bareyre et al., 2005), leading us to examine the proportion of $vG1^{+}$ boutons that derive from CST neurons. To assess this, we crossed a forebrain restricted *Emx1::*Cre line with a *Thy1::Φ*YFP reporter. At p21 we found that

2.0 ± 0.4% (n = 232; 2 mice) of $vG1^+$ terminals in the ventral spinal cord expressed YFP (Figure S2I, J), and few, if any of these contacted motor neurons.

(D, E) $vG1^+$ proprioceptive sensory terminals that contact GFP^+ motor neurons in p21 *Hb9::*GFP mice express the synaptic vesicle proteins Syn1 (D) and SV2 (E).

(F, G) $vG1^+$ proprioceptive sensory terminals are aligned with motor neuron domains that cluster the AMPA receptor subunits GluR2/3 (F) and PSD95 (G).

Figure S2

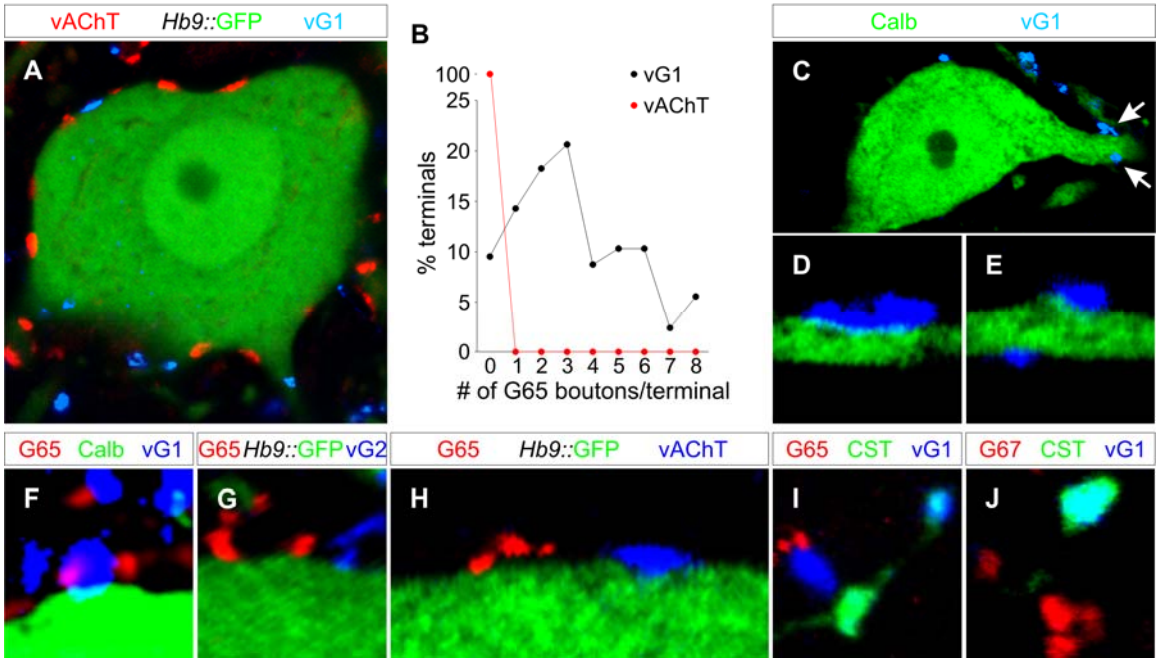

Figure S2. Specificity of GABApre contacts with proprioceptive sensory terminals

(A) GFP^{+} motor neurons in *Hb9::*GFP mice receive excitatory vAChT^{+} 'C' bouton inputs from cholinergic interneurons in addition to vGlut1^{+} inputs from sensory neurons.

(B, H) Cholinergic vAChT^{+} 'C' terminals on motor neurons are not contacted by GAD65 (G65)$^{+}$ boutons.

(C-E) Proximal dendrites of Calbindin (Calb)$^{+}$ Renshaw cells receive input from vGlut1 (vG1)$^{+}$ proprioceptive sensory terminals (arrows in C).

(F) vG1^{+} proprioceptive sensory terminals that contact Calb^{+} Renshaw cells receive input from G65^{+} boutons.

(G) G65^{+} boutons do not contact vGlut2 (vG2)$^{+}$ excitatory interneuron terminals on GFP-labeled motor neurons in *Hb9::*GFP mice.

(I, J) In p21 *Emx1::*Cre *; Thy1:: Φ*YFP mice, the majority of YFP^{+} CST boutons around motor neurons lack vG1 expression. None of the CST derived boutons, regardless of vG1 expression status, are contacted by G65^{+} (I) or GAD67 (G67)+ (J) GABAergic boutons, even though a neighboring YFP^{off} vG1 sensory terminal is contacted by several G65^{+} boutons.

Figure S3

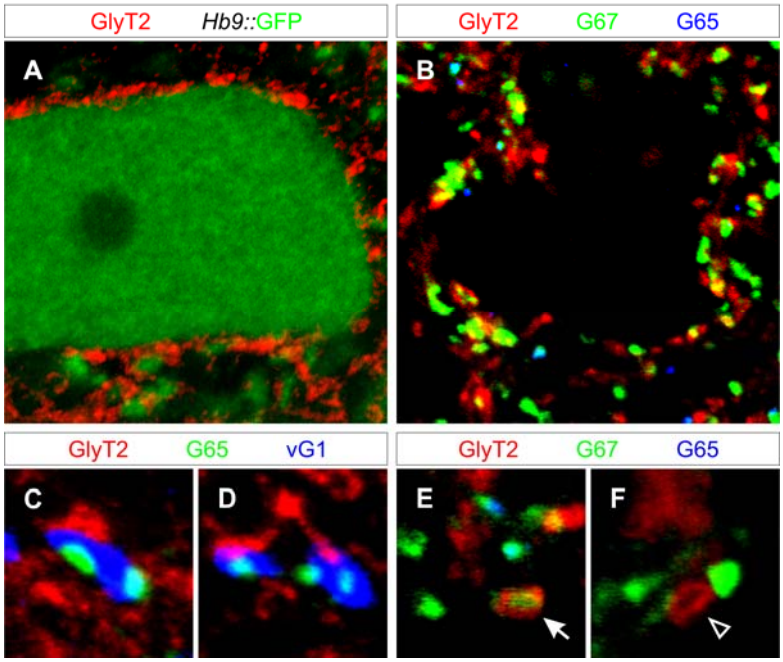

Figure S3. Inhibitory synaptic contacts with motor neurons

(A) GlyT2^{+} glycinergic boutons on *Hb9::*GFP^{+} motor neurons in p21 mice.

(B) GAD67 (G67) but not GAD65 (G65) is expressed in a subset of GlyT2^{+} glycinergic boutons on motor neurons (black holes).

(C, D) G65^{+} boutons on vGlut1^{+} sensory terminals lack GlyT2 expression.

(E, F) Some GlyT2^{+} boutons express G67 but not G65 (arrow in E), or neither of the two GAD isoforms (arrowhead in F).

Based on these analyses, four molecularly distinct inhibitory terminals exist in the vicinity of motor neurons (% of all inhibitory boutons around motor neurons): i. boutons expressing GlyT2 but not G67 or G65 (33%), ii. boutons that co-express GlyT2 and G67 but not G65 (31%), iii. boutons that express G67 but not GlyT2 or G65 (24%), and iv. boutons that express G65 and G67 but not GlytT2 (12 %) (n = 3 mice).

Figure S4

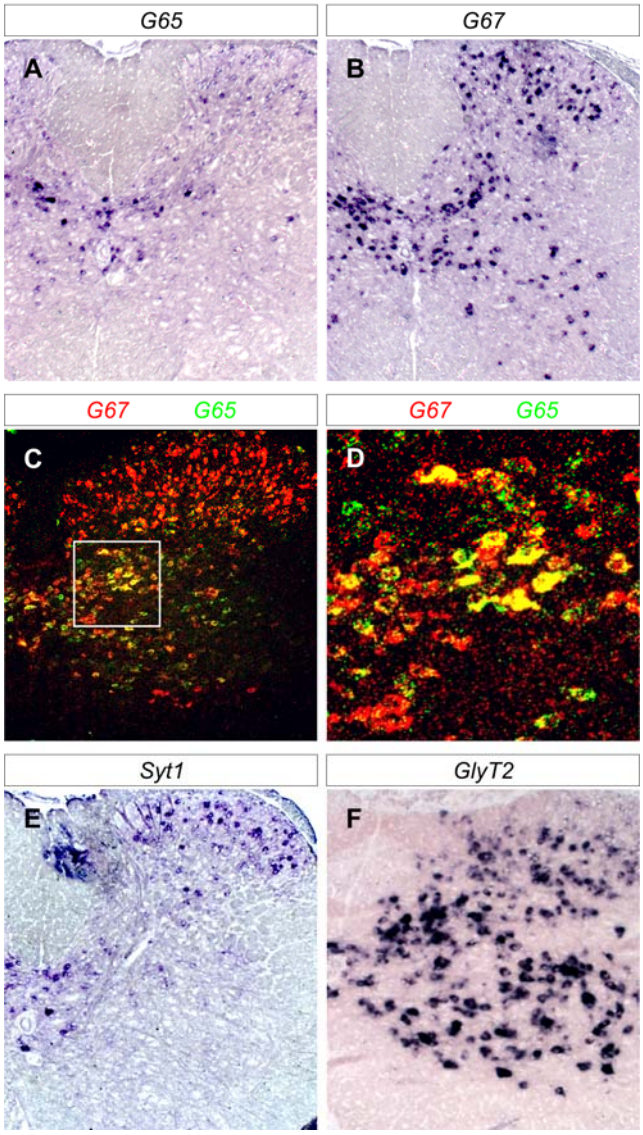

Figure S4. Mapping the source of GABApre boutons in post-natal lumbar spinal cord

(A) Neurons expressing *Gad65 (G65)* transcript are concentrated in the medial region of the deep dorsal horn in p6 to adult mice. Image (A) of p30 lumbar spinal cord.

(B) Neurons expressing *Gad67 (G67)* transcript are widely distributed in the dorsal and ventral halves of the spinal cord of p6 to adult mice. Image (B) of p30 lumbar spinal cord.

(C) Fluorescent double *in situ* hybridization histochemistry shows that neurons co-expressing *G67* (red) and *G65* (green) are concentrated in the medial region of the deep dorsal horn in p6 mice.

(D) High magnification image of medial dorsal horn (boxed domain in C), showing neurons that co-express *G67* and *G65*.

(E) *Syt1* is also expressed by neurons in the medial region of the deep dorsal horn in p15 to adult mice. Image (E) of p30 lumbar spinal cord.

(F) *GlyT2* is expressed by neurons throughout the spinal cord of p6 to adult mice. Image (F) of p30 lumbar spinal cord.

Figure S5

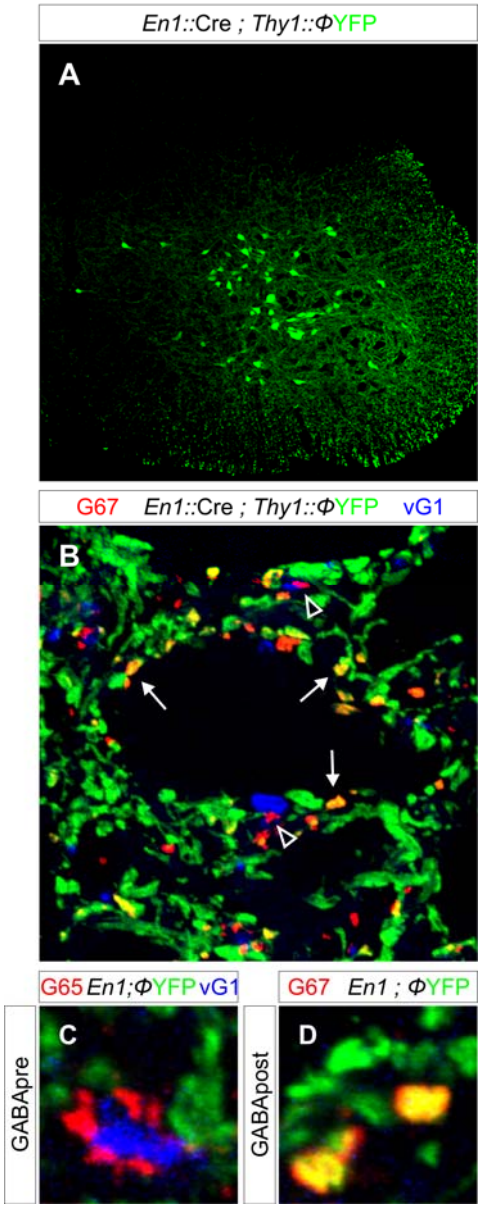

Figure S5: GABApost terminals derive from *En1*-expressing interneurons

(A) Ventral restriction of YFP^{+} neurons in *En1::*Cre *; Thy1::Φ*YFP mice.

(B) *En1::*Cre *; Thy1::Φ*YFP marked axons and terminals (subset of motor neuron region in A). GAD67 (G67) is expressed in a subset of YFP^{+} boutons (arrows) that contact motor neurons (black holes). G67^{+} boutons in contact with vG1^{+} terminals (arrowheads) lack YFP expression.

(C) Fewer than 0.001% of YFP-labeled GABApost axons in *En1::*Cre *; Thy1::Φ*YFP mice contact vG1^{+} sensory terminals.

(D) In *En1::*Cre *; Thy1::Φ*YFP mice, $G67^{+}$ boutons on motor neurons express YFP. 76.9 ± 2.2% (n = 603 boutons; 2 mice) of $G67^{+}$, $GAD65^{off}$ boutons are GFP^{+} in the *En1::*Cre *; Tau::Φ*mGFP cross.

We conclude that GABApre and GABApost interneurons have distinct transcriptional provenances.

Figure S6

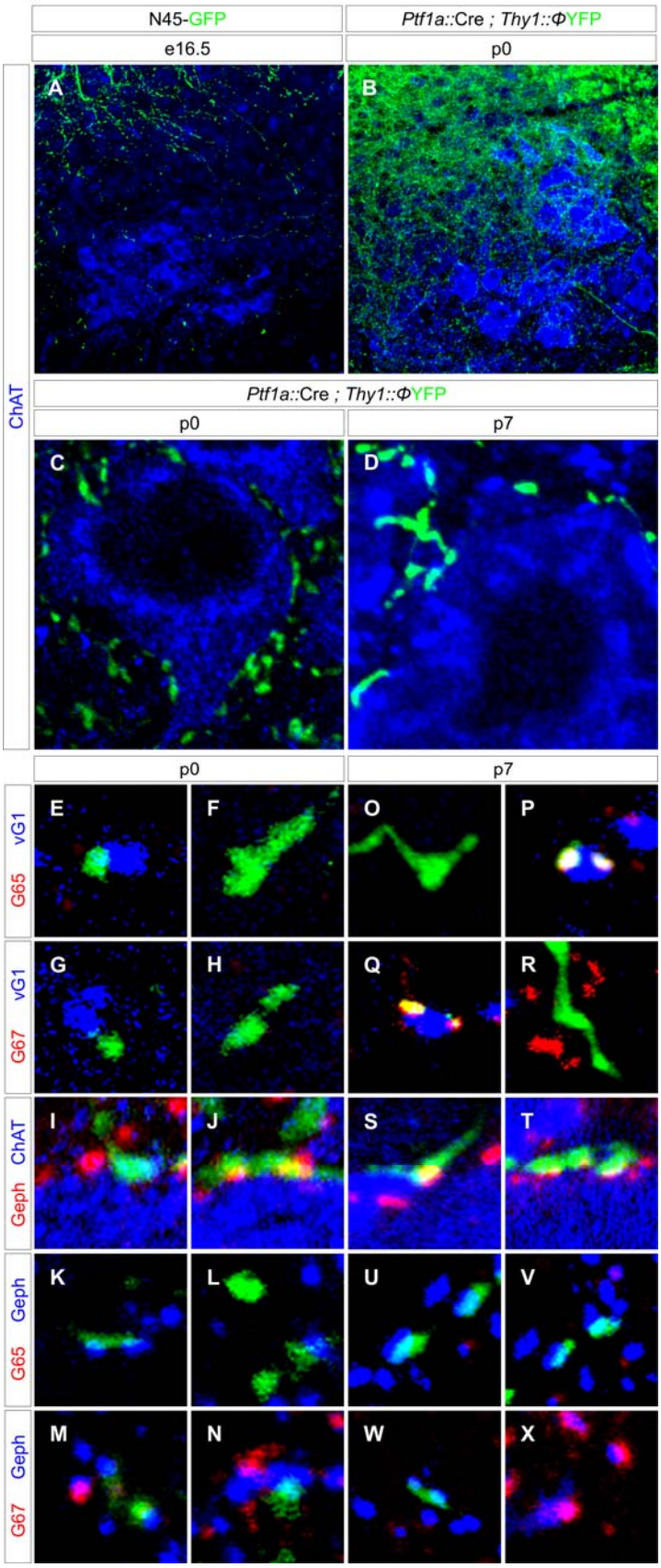
N45-GFP
Ptf1a::Cre ; Thy1::ΦYFP
e16.5
p0
ChAT
A
B
Ptf1a::Cre ; Thy1::ΦYFP
p0
p7
C
D
p0
p7
vG1
G65
E
F
O
P
vG1
G67
G
H
Q
R
ChAT
Geph
I
J
S
T
Geph
G65
K
L
U
V
Geph
G67
M
N
W
X

Figure S6. Developmental time course of GABApre synapse formation

We performed this developmental analysis in *Gad65::*^{N45}GFP and *Ptf1a::*Cre *; Thy1::Φ*YFP mice and find a similar time course of GABApre synapse formation in both strains. The panels display representative images for these time points in *Ptf1a::*Cre *; Thy1::Φ*YFP mice (except panel A showing *Gad65::*^{N45}GFP spinal cord).

(A-D) FP^+ GABApre terminals can be seen in the vicinity of the motor pool region at e16.5 (A) and in contact with $ChAT^+$ motor neurons at p0 to p7 (B-D). (C, D) are high magnification images of a single motor neuron.

(E-N) At p0 to p2 FP^+ axons contact motor neurons and sensory terminals, however do not express high levels of pre-synaptic GAD65 (G65) (E, F) and GAD67 (G67) (G, H) even though they occasionally contact motor neuron $Geph^+$ puncta (I-N).

(O-X) At p7 FP^+ axons contact motor neurons and sensory terminals, however only contacts with sensory terminals express high levels of G65 (P) and G67 (Q) even though many FP^+ axons contact motor neuron $Geph^+$ puncta (S-X).

Figure S7

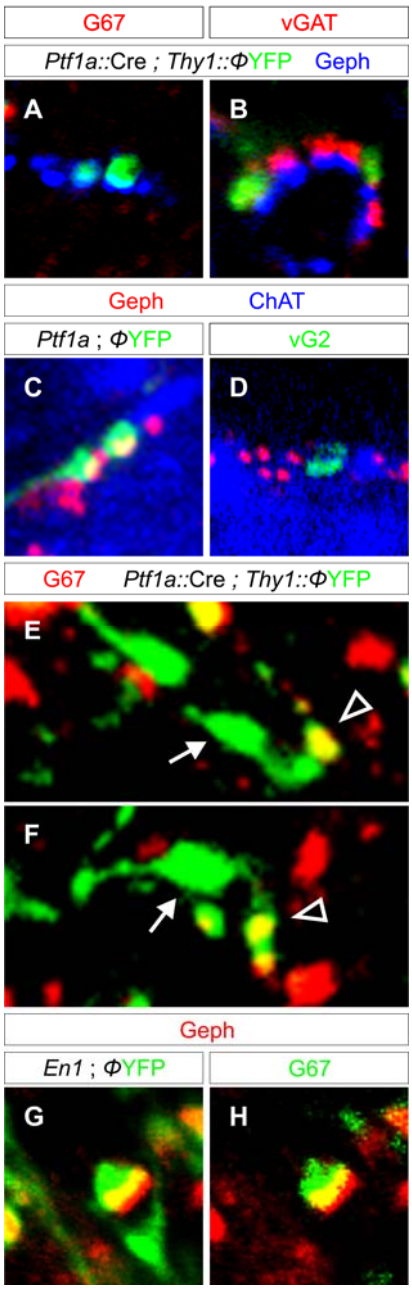

Figure S7. Characterization of GABApre and GABApost contacts with motor neurons

(A, B) In p15 *Ptf1a::*Cre *; Thy1::Φ*YFP mice, both YFP^{+} GABApre axonal varicosities and YFP^{off}, GAD67 (G67)$^{+}$, vGAT^{+} GABApost boutons align with motor neuron Geph^{+} puncta. Note YFP^{+} GABApre axonal varicosities do not cluster markers of pre-synaptic differentiation such as G67 (A) or vGAT (B) while neighboring YFP^{off} GABApost synapses express normal levels of pre-synaptic proteins (B).

(C, D) In p15 *Ptf1a::*Cre *; Thy1::Φ*YFP mice, YFP^+ GABApre varicosities, but not vGlut2 (vG2)+ excitatory boutons align with $Geph^+$ puncta of $ChAT^+$ motor neurons.

(E, F) In p15 *Ptf1a::*Cre *; Thy1::Φ*YFP mice, G67 expression is restricted to compact GABApre boutons (arrowheads) but absent from larger varicosities (arrows). Note that the compact GABApre boutons and larger varicosities are found in a single axonal process.

(G, H) In p21 *En1::*Cre *; Thy1::Φ*YFP mice, YFP^+, $G67^+$ GABApost boutons are aligned with $Geph^+$ puncta. Image of same bouton in G and H.

Figure S8

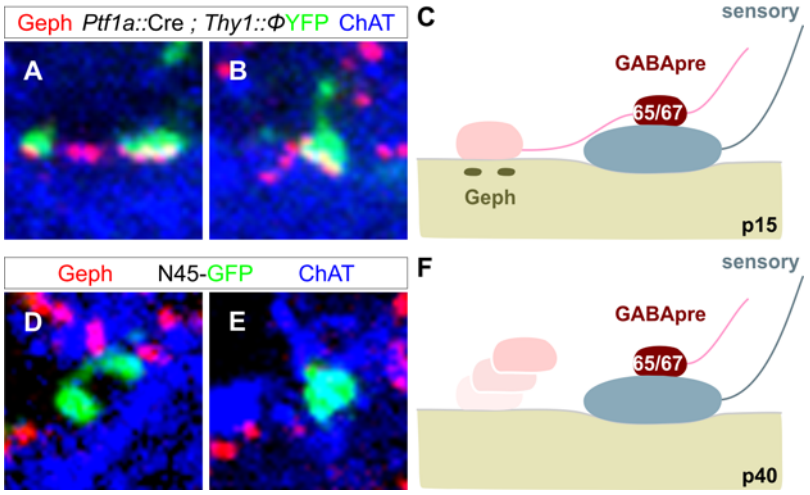

Figure S8. Developing GABApre axonal contacts with motor neurons are transient

(A-B) In p15 *Ptf1a::*Cre *; Thy1::Φ*YFP mice, YFP^{+} GABApre axonal varicosities contact $ChAT^{+}$ motor neurons (blue) and are often (~50%) aligned with post-synaptic $Geph^{+}$ clusters (red).

(C) Schematic showing GABApre axons at p15 contacting sensory terminals and completing pre-synaptic differentiation (accumulation of GAD65, GAD67). GABApre axons also contact motor neurons and cluster Geph post-synaptically without any pre-synaptic differentiation (Figure 3G).

(D-E) In p40 *Gad65::*^{N45}GFP mice, $^{N45}GFP^{+}$ GABApre axonal varicosities are occasionally seen in contact with motor neurons, however they lack post-synaptic Geph.

(F) Schematic of the mature GABApre axonal and synaptic arrangement.

We conclude that by p40, transient axonal contacts of GABApre neurons with motor neurons are removed leaving only the fully differentiated GABApre synapses on sensory terminals and their axons.

Figure S9

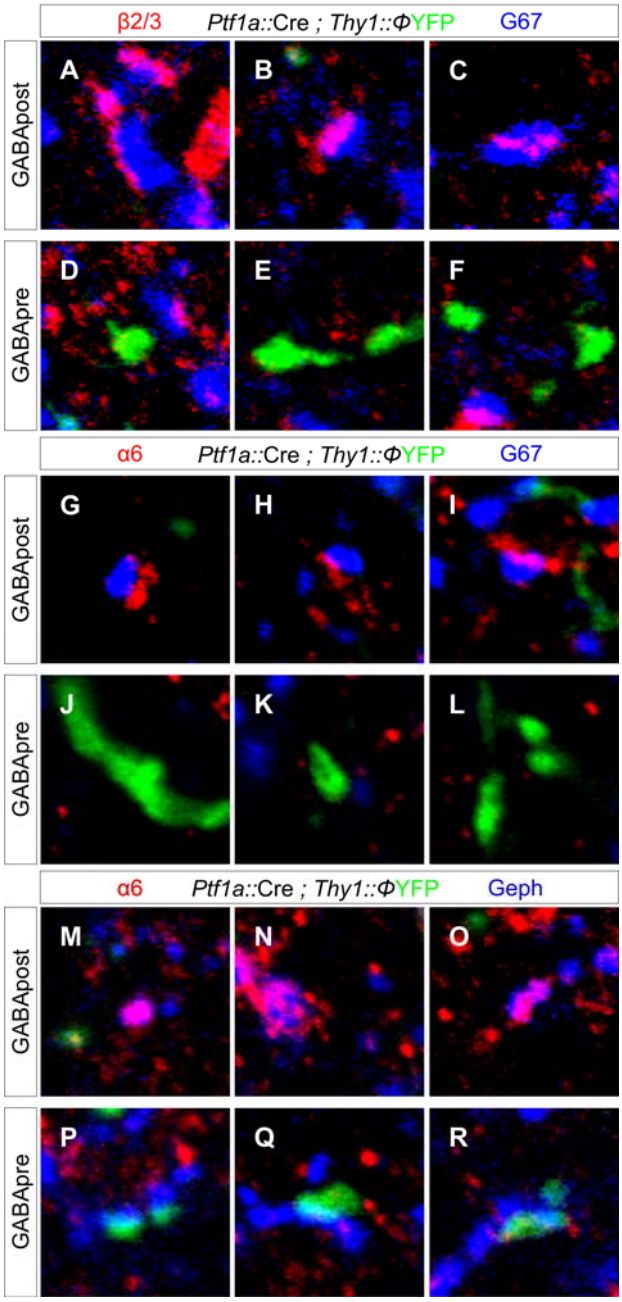

Figure S9. $GABA_A$ receptor distribution at GABApre and GABApost contacts with motor neurons

(A-C) In p15 *Ptf1a::*Cre *; Thy1::Φ*YFP mice, GAD67 $(G67)^+$, YFP^{off} GABApost boutons align with post-synaptic $GABA_A$ receptor β2/3 subunits.

(D-F) In p15 *Ptf1a::*Cre *; Thy1::Φ*YFP mice, YFP^+ GABApre axonal varicosities are not seen in alignment with post-synaptic GABA(A) receptor β2/3 subunits.

(G-I) In p15 *Ptf1a::*Cre *; Thy1::Φ*YFP mice, $G67^{+}$, YFP^{off} GABApost boutons align with post-synaptic $GABA_A$ receptor α6 subunit.

(J-L) In p15 *Ptf1a::*Cre *; Thy1::Φ*YFP mice, YFP^{+} GABApre axonal varicosities are not seen in alignment with post-synaptic $GABA_A$ receptor α6 subunit.

(M-O) In p15 *Ptf1a::*Cre *; Thy1::Φ*YFP mice, $Geph^{+}$ boutons not in alignment with pre-synaptic YFP varicosities (GABApost boutons) co-express post-synaptic $GABA_A$ receptor α6 subunit.

(P-R) In p15 *Ptf1a::*Cre *; Thy1::Φ*YFP mice, $Geph^{+}$ boutons in alignment with pre-synaptic YFP varicosities (GABApre axonal varicosities) do not co-express post-synaptic $GABA_A$ receptor α6 subunits. We conclude that GABApre axonal varicosities in contact with motor neurons do not cluster GABA receptors and only some synapses undergo the initial and transient post-synaptic differentiation step of clustering Geph.

Figure S10

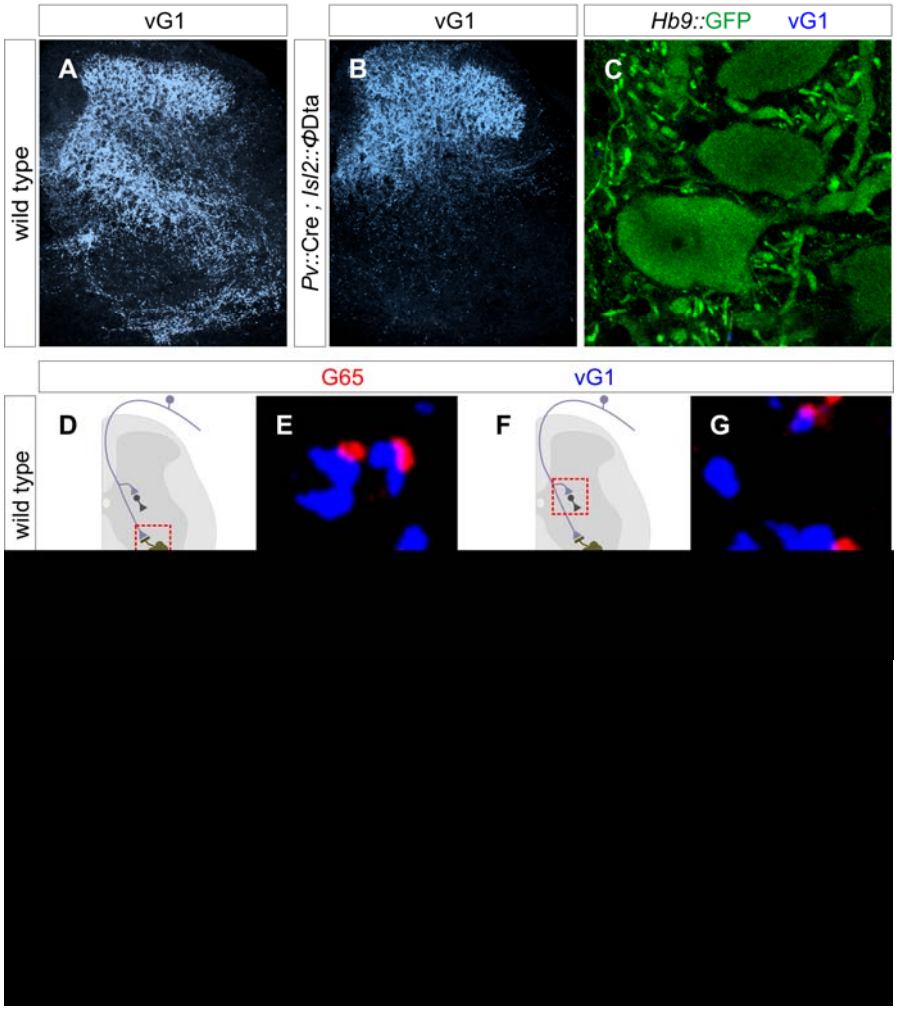

Figure S10. Loss of proprioceptive sensory terminals and GABApre boutons in *Pv::*Cre *; Isl2::Φ*Dta mice

(A) vGlut1 (vG1) expression in wild type p21 lumbar spinal cord.

(B) vG1 expression in p21 lumbar spinal cord of *Pv::*Cre *; Isl2::Φ*Dta mice. In *Pv::*Cre *; Isl2::Φ*Dta mice proprioceptive sensory neurons are absent from the DRG (data not shown). In contrast to *Er81* mutants, $vG1^+$ terminals are depleted from the intermediate as well as ventral spinal cord.

(C) Almost complete absence (1.8% of wild type) of $vG1^+$ terminals in the vicinity of GFP-labeled motor neurons in p21 *Pv::*Cre *; Isl2::Φ*Dta*; Hb9::*GFP mice.

(D-O) Comparison of changes in pattern of vG1 and GAD65 (G65) expression in the spinal cords of wild type, $Er81^{-/-}$ and *Pv::*Cre *; Isl2::Φ*Dta mice. In *Er81* mutants, $vG1^+$ and $G65^+$ boutons are lost from the

ventral but not intermediate spinal cord (I, K). In *Pv::*Cre *; Isl2::Φ*Dta mice vG1^{+} sensory terminals and G65^{+} boutons are lost from both ventral and intermediate spinal cord (M, O). Schematics (D, F, H, J, L, N) show region (red box) where image was acquired in corresponding panel.

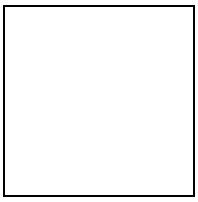

Figure S11. Reduction in axonal and synaptic ^{N45}GFP fusion protein expression in *Gad65::*^{N45}GFP ; *Er81*$^{-/-}$ mice

(A, B) ^{N45}GFP expression in the spinal cord of wild type (A) and *Er81*$^{-/-}$ (B) mice at p15. Note the presence of a few ectopic, scattered, ^{N45}GFP-labeled neurons in the ventral spinal cord in *Er81* mutants. See Figure 7 for a full characterization of the *Gad65::*^{N45}GFP mouse and the determination that it exclusively labels GABApre boutons.

(C) Quantitation of somatic ^{N45}GFP levels in individual neurons of the medial region of the deep dorsal horn (rectangle in A and B). Loss of proprioceptive sensory terminals does not effect expression of ^{N45}GFP in GABApre neurons ($p > 0.7$ Mann Whitney U Test; $n > 100$ neurons; 3 mice). We also find that endogenous levels of *Gad65 (G65)* appear normal by *in situ* hybridization histochemistry (data not shown).

(D, E) ^{N45}GFP expression levels in axons and varicosities in the ventral spinal cord of wild type and *Er81*$^{-/-}$ mice at p15. Images of dashed box region in A and B.

(F) Quantitation of ^{N45}GFP levels in GABApre boutons in the ventral spinal cord of wild type and *Er81*$^{-/-}$ mice. We find a significant decrease of ^{N45}GFP in *Gad65::*^{N45}GFP *; Er81*$^{-/-}$ mice ($p < 0.0001$ Mann Whitney U Test, $n > 100$ boutons; 3 mice)

(G-I) G65 and ^{N45}GFP expression at individual vGlut1^{+} sensory terminals in the ventral horn of p15 *Gad65::*^{N45}GFP and *Gad65::*^{N45}GFP *; Er81*$^{-/-}$ mice.

(J, K) In *Ptf1a::*Cre ; *Thy1Φ*YFP ; *Er81*$^{-/-}$ mice, YFP levels are maintained in ventral GABApre axons and varicosities, despite the loss of sensory terminals.

We conclude that the trafficking of ^{N45}GFP to GABApre axonal varicosities is defective in the absence of sensory terminals, reflecting the deficit of endogenous G65 in synaptic boutons.

Figure S12

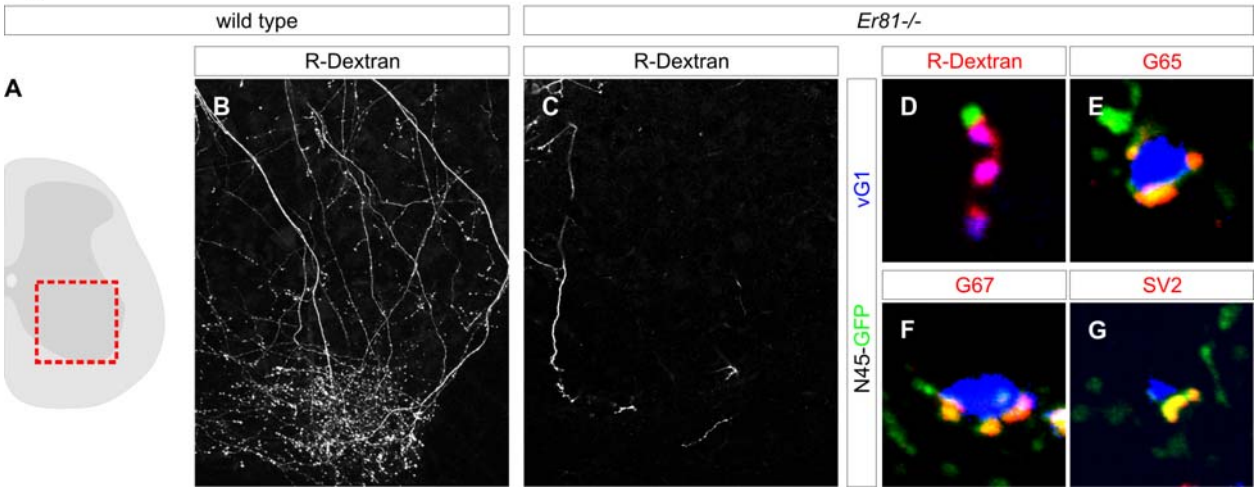

Figure S12. GABApre boutons contact the few proprioceptive axons that reach the ventral spinal cord in *Er81* mutants

(A) Region of analysis in B-G.

(B, C) Application of Rhodamine-Dextran (R-Dextran) to dorsal roots labels proprioceptive axons projecting to the ventral spinal cord. In p15 *Er81*$^{-/-}$ mice, very few axons are found in the ventral spinal cord.

(D) In *Gad65::*^{N45}GFP ; *Er81*$^{-/-}$ mice vGlut1 (vG1)$^{+}$ terminals are filled by R-Dextran and are contacted by ^{N45}GFP^{+} boutons.

(E) In *Gad65::*^{N45}GFP ; *Er81*$^{-/-}$ mice a ventral vG1^{+} proprioceptive terminal is contacted by GAD65 (G65)+, ^{N45}GFP^{+} boutons.

(F, G) In *Gad65::*^{N45}GFP ; *Er81*$^{-/-}$ mice ventral vG1^{+} proprioceptive terminals are contacted by GAD67 (G67)+, ^{N45}GFP^{+} (F) and SV2^{+}, ^{N45}GFP^{+} (G) boutons.

Figure S13

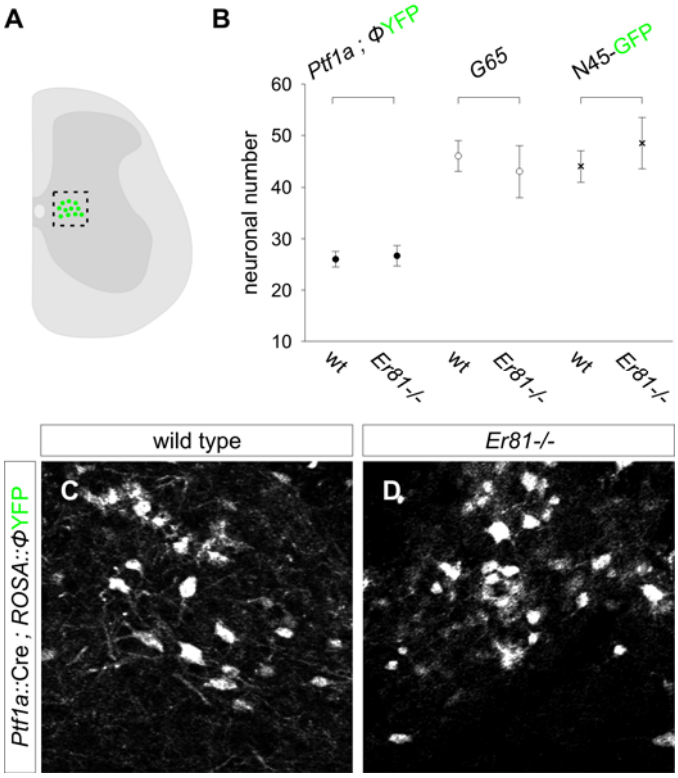

Figure S13. GABApre neurons survive in *Er81* mutants

(A) Region of analysis in B-D.

(B) Quantitation of labeled neurons in medial region of deep dorsal horn in wild type and *Er81*$^{-/-}$ mice. First grouping compares *Ptf1a::*Cre *; ROSA::Φ*YFP neurons, second grouping compares *Gad65* expressing neurons, third grouping compares $^{N45}GFP^{+}$ neurons.

(C, D) In *Ptf1a::*Cre *; ROSA::Φ*YFP ; *Er81*$^{-/-}$ mice, YFP-labeled neurons are detected at normal numbers in the medial region of the deep dorsal horn.

Figure S14

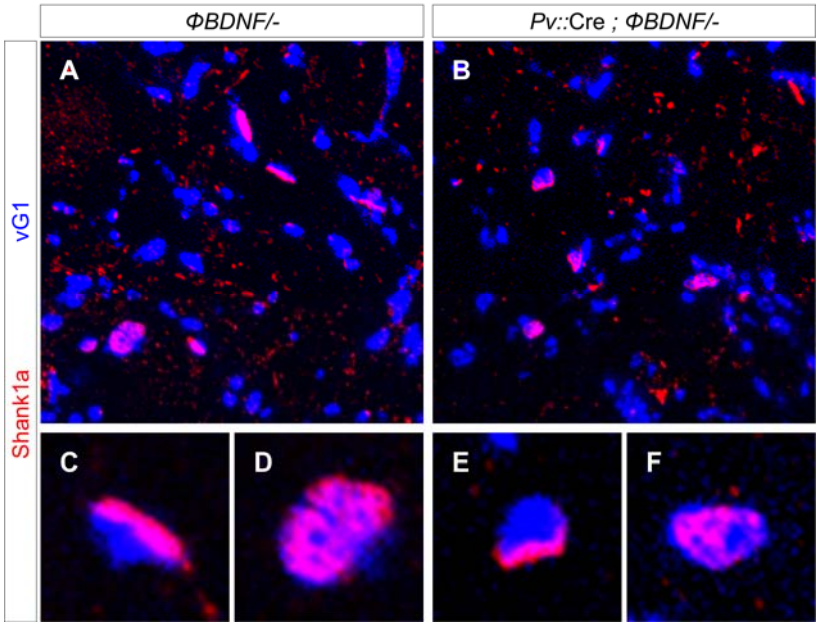

Figure S14. Proprioceptive sensory neurons form synaptic contact with motor neurons in the absence of sensory-derived BDNF signaling

(A, C, D) Shank1a expression aligns with vGlut1 $(vG1)^{+}$ proprioceptive sensory terminals in p21 *ΦBDNF/-* (control) mice.

(B, E, F) Shank1a expression still aligns with $vG1^{+}$ proprioceptive sensory terminals in p21 *Pv::*Cre *;* *ΦBDNF/-* mice, which lack proprioceptor BDNF activity.

Figure S15

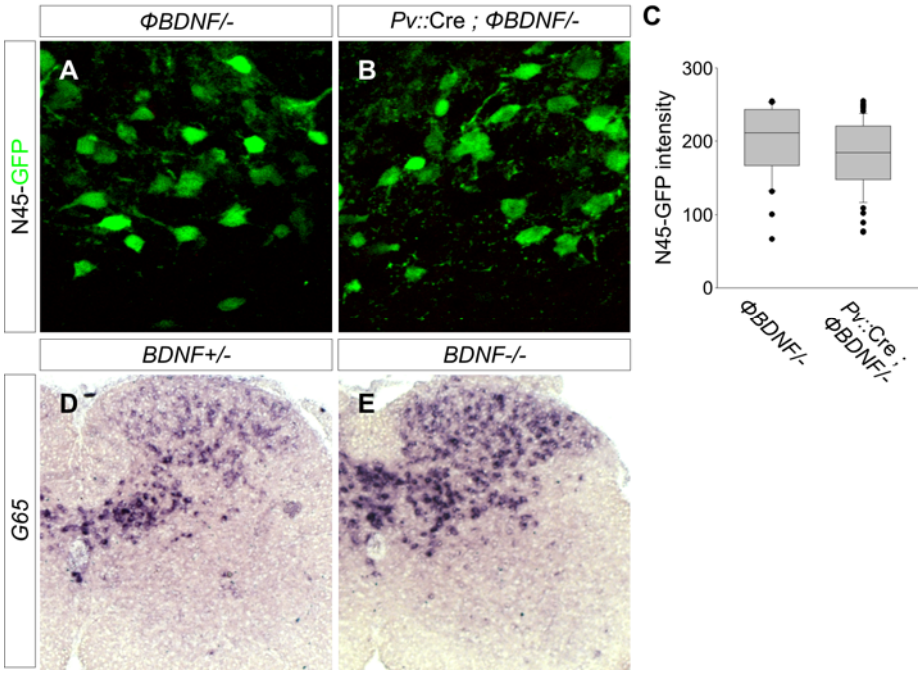

Figure S15. Survival of GABApre neurons in the absence of BDNF signaling

(A-C) In *Gad65::*^{N45}GFP mice, the number of GFP-labeled neurons in the medial region of the deep dorsal horn (presumptive GABApre neurons) is unaffected by the loss of proprioceptor BDNF signaling. (C) shows that ^{N45}GFP intensity in individual GABApre neurons is not changed by the loss of proprioceptor BDNF (*Pv::*Cre *; ΦBDNF/-)*, suggesting BDNF does not regulate the transcription or translation of GAD65 (G65). Quantitation shown with median and 95% confidence limits ($p > 0.6$ Mann Whitney U Test; n >100 neurons; 3 mice).

(D, E) Persistence of *G65* expression in the medial region of deep dorsal horn in wild type and constitutive *BDNF* mutants, assayed at p15.

Figure S16

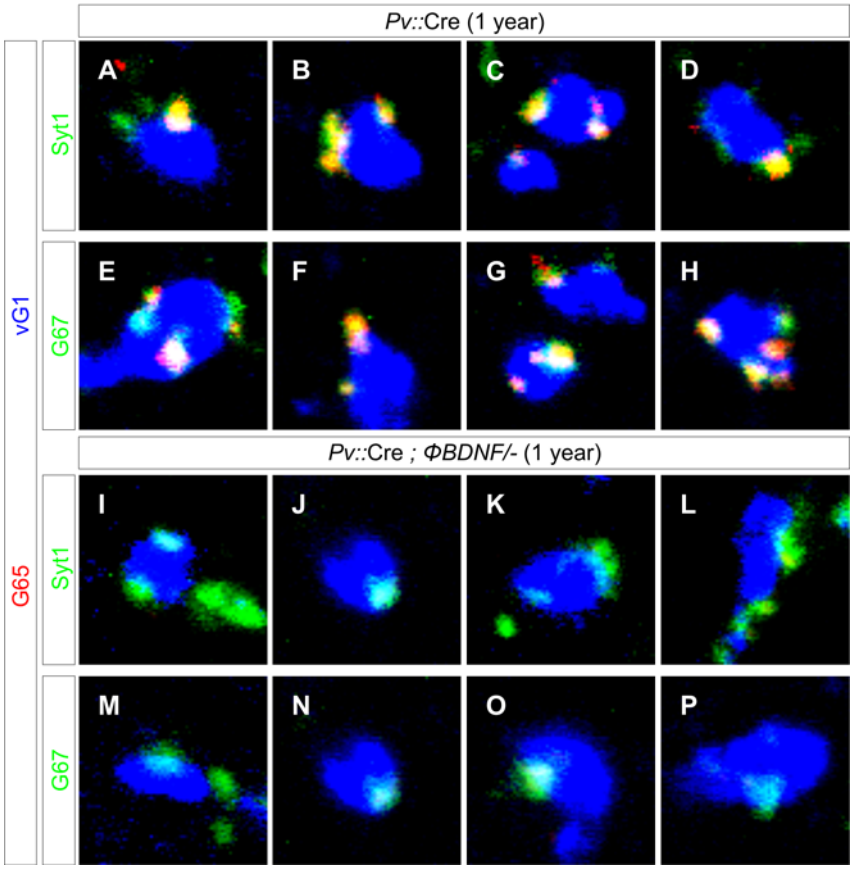

Figure S16. Sensory derived *BDNF* is not required for GABApre synaptic maintenance in adult mice

(A-D) In >1 year-old *Pv::*Cre mice, vGlut1 (vG1)$^{+}$ sensory terminals are studded with Syt1^{+} GABApre boutons that express high levels of GAD65 (G65).

(E-H) In >1 year-old *Pv::*Cre mice, vG1^{+} sensory terminals are studded with GAD67 (G67)$^{+}$ GABApre boutons that express high levels of G65.

(I-L) In >1 year-old *Pv::*Cre *; ΦBDNF/-* mice, vG1^{+} sensory terminals are studded with Syt1^{+} GABApre boutons that lack high levels of G65.

(M-P) In >1 year-old *Pv::*Cre *; ΦBDNF/-* mice, vG1^{+} sensory terminals are studded with G67^{+} GABApre boutons that lack high levels of G65.

We conclude that GABApre terminals are maintained throughout the life of animals lacking sensory derived *BDNF,* however these terminals fail to accumulate G65.

Figure S17

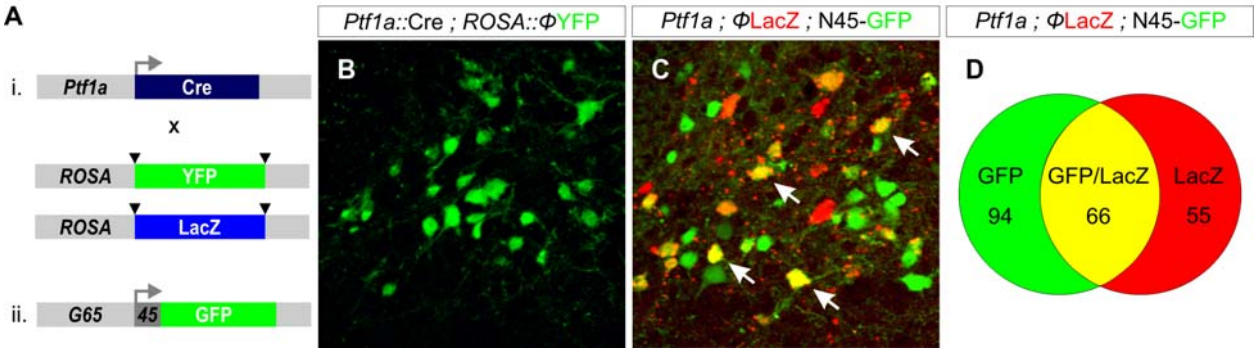

Figure S17. Identification of GABApre neurons in the medial region of deep dorsal horn

(A) Mouse lines used for analysis.

(B) YFP-labeled cells in *Ptf1a::*Cre *; ROSA::Φ*YFP mice in the medial region of deep dorsal horn.

(C) In *Gad65::*^{N45}GFP ; *Ptf1a::*Cre *; ROSA::*LacZ mice, neurons that co-express YFP and LacZ are likely to be GABApre neurons (arrows in C), based on the high percentage of GABApre boutons that labeled in *Ptf1a::*Cre *; Tau::Φ*mGFP and *Gad65::*^{N45}GFP tracings (see Figures 3, 7).

(D) Fraction of GFP/LacZ double positive neurons as a function of GFP and LacZ single positive in *Gad65::*^{N45}GFP ; *Ptf1a::*Cre *; ROSA::*LacZ mice. 55% of LacZ^{+} neurons co-expressed GFP, and 33% of GFP^{+} neurons co-expressed LacZ.

Figure S18

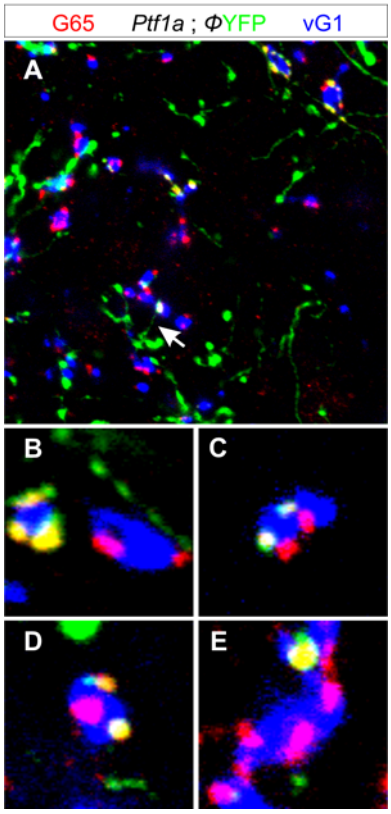

Figure S18. Mosaic analysis of GABApre bouton contacts with vGlut1^{+} proprioceptive sensory terminals

(A) In *Ptf1a::*Cre *; Thy1::Φ*YFP (line 15) mice, mosaic expression results in YFP expression in ~30% of GABApre boutons. In these mice, GAD65 (G65) is expressed in GABApre axonal domains that contact vGlut1 (vG1)$^{+}$ proprioceptive sensory terminals. Arrow points to one GABApre axon that forms a compact GABApre bouton on a vG1^{+} proprioceptive sensory terminal and also forms a larger varicosity nearby, presumably with a motor neuron dendrite.

(B-E) Panels show that vG1^{+} proprioceptive sensory terminals are contacted by G65^{+} GABApre boutons, only some of which express YFP. Thus GABApre boutons contacting an individual vG1^{+} proprioceptive sensory terminal typically derive from more than one GABApre neuron.

Table S1. Gene expression profiles in mouse spinal cord and/or dorsal root ganglia

A. Genes implicated in GABAergic synaptic differentiation

Neuroligin 1
Neuroligin 2
Neuroligin 3
Neurexin
BDNF
TrkC
AnkG
Neurofascin

B. Genes implicated in any aspect vertebrate synaptic differentiation

Sidekick 1
Sidekick 2
GDNF
CNTF
NGF
NT3
TrkA
TrkB
L1
CHL1
NrCAM
NCAM1
NCAM2
DSCAM
Dascaml1
Neph1-3
Nephrin
Nectin 1-4
Nectin Like 1-5
Contactin 1-6
Caspr 1-5
IgLON family (Cepu-1, Negr1, Lamp, OBCAM)

The expression profile of the genes listed above was determined by *in situ* hybridization histochemistry on cryostat sections of p6 spinal cord and DRG. With the exception of *BDNF*, none of the genes exhibited sensory neuron or GABApre selective profiles of expression.